



The Effect of Environmental Parameters on the Corrosion Behavior of Simple Shear Extruded AZ91 Magnesium Alloys

Ramineh Medhat^{a,1}, Mahmoud Pakshir^{a,2,*}, Khashayar Morshed Behbahani^{a,1}, Pooria Najafisayar^{a,3}

^aDepartment of Materials Science and Engineering, Shiraz University, Shiraz, Iran

¹MS of Corrosion and Protection of Metals, Dept. of Materials Science and Engineering, Shiraz University

² Prof. of Materials Science and Engineering Department, Shiraz University

³ Assistant Prof. of Materials Science and Engineering Department, Shiraz University

Abstract

In this study, the effects of forming method (extrusion) and environmental factors (solution pH and temperature) on the corrosion performance of AZ91 magnesium alloys were investigated using potentiodynamic polarization, electrochemical impedance spectroscopy (EIS), scanning electron microscopy (SEM) and salt spray techniques. The polarization test results of the specimens showed that simple shear extrusion (SSE) process have adverse effect on the samples corrosion behavior in 3.5 wt% NaCl solution and corrosion current densities increased by increasing temperature/ decreasing pH of the solution. Moreover, the EIS test results showed that the increase in temperature or acidity of the solution led to decrease in charge-transfer resistance (R_{ct}) at the electrode/solution interface for both as-cast and SSEd samples. In addition, the weight loss measurements, based on the salt spray test results, revealed that normally extruded samples have better corrosion performance than as-cast and SSEd ones which is in accordance with the electrochemical test results.

Keywords: AZ91 magnesium alloy; Simple shear extrusion; Corrosion, Electrochemical impedance spectroscopy, Potentiodynamic test

1. Introduction

Severe plastic deformation (SPD) technique is regarded as suitable grain refining method to improve mechanical behavior of metallic materials [1, 2]. Many SPD techniques have been proposed throughout the literature such as equal-channel angular pressing (ECAP) [3, 4], high pressure torsion

(HPT) [5] and accumulative roll bonding (ARB)[1, 6] to fabricate ultra-fine grained (UFG) and nano-crystalline materials. Among these SPD methods, simple shear extrusion is one of the modern techniques to produce such materials by imposing high strain values via pressing the sample through a channel in which the specimen deforms gradually with a constant cross-section area [7].

Magnesium and its alloys are commonly used for different industrial applications owing to their low specific weights and

*Corresponding Author

E-mail address: pakshir@shirazu.ac.ir

high strength/weight ratio[8]; but their applications are restricted due to their poor corrosion resistance. The corrosion behavior of magnesium alloys have been investigated in the previous studies to some extent. The main proposed corrosion mechanisms of Mg alloys are general corrosion and pitting attack. General corrosion is the predominant mechanism at beginning stages while pitting attack occurs at longer times and the surface attack is controlled by three surface state variables namely the formation of $Mg(OH)_2$, precipitation of $MgAl_2(SO_4)_4 \cdot 2H_2O$ and finally formation of metastable Mg^+ concentration areas [9]. Moreover, it has been reported that magnesium alloys exhibit corrosion and passivation zones in dilute NaCl solutions with corrosion products including $Mg(OH)_2$, $Mg_5(CO_3)_4(OH)_2 \cdot 8H_2O$ and MgO while the two latter phases are present on their surface as passive film[10].

It has been reported that the grain size and its distribution[11], residual stresses[12], texture[12, 13] and composition[14] of the metals may influence their corrosion behavior. In fact, chemical composition of Mg alloys, applied bulk deformation methods (like ECAP or SSE) and environmental parameters (like type of the corrosion medium, temperature and pH) have pronounce effect on their corrosion behavior. The effect of such factors has been investigated through the literature. For example, it has been reported that the corrosion behavior of magnesium alloys is affected by grain size and twins that are presented in the alloy microstructure[13]. In addition, Ma et al.[15] showed that the bulk ultrafine grained AZ91D magnesium alloy, fabricated via ECAP technique, have impaired

corrosion performance owing to activated α -phase matrix and propagation of β -phase in the α -phase matrix.

Recently, the effect of alloying elements concentration (like Zn and Mn) on the corrosion behavior of Mg alloys has been reported [16-18]. Although there are many studies about the microstructure variation and mechanical properties of the Mg alloys but the effects of processing parameters (specially SSE process) and environmental factors (like pH and temperatures) on the corrosion behavior of such alloys have not been investigated enough in the literatures.

In this study, electrochemical techniques and salt spray method were used to investigate the effect of extrusion on the corrosion performance of AZ91 alloys. In addition, the effects of temperature and pH on the corrosion behavior of as-cast and SSEed AZ91 Mg alloys were evaluated in the 3.5 wt% NaCl solution using polarization tests and electrochemical impedance spectroscopy.

2. Experimental procedure

Billets of AZ91 magnesium alloy, with dimensions of $30 \times 30 \times 20$ mm and nominal composition shown in Table.1, were used to produce SSEed samples. Before the SSE process, the AZ91 billets were heat-treated consecutively at 270 and 415°C for 2 and 24 h, respectively. The heat treated samples were then extruded at 415°C using screw press with ram speed of 0.2 mm/s. In the next step, the samples were cut in rectangular shape with cross section of 1 cm², mechanically polished with SiC abrasive paper up to 3000 grade and finally washed with distilled water and ethanol

Table 1: Chemical composition of AZ91 alloy (wt.%).

Al	Zn	Mn	Fe	Be	Si	Cu	Ni
9.05	0.65	0.21	0.0021	0.00082	0.022	0.002	0.00057

to prepare them for the corrosion tests.

All the electrochemical experiments were conducted in 3.5 wt% NaCl solution (at temperature range from 25 °C to 60 °C and pH range from 3 to 12) with a μ Autolab3 system and the results were analyzed using GPES and FRA 4.9 software. The effect of solution temperature on the corrosion behavior was investigated in pure 3.5 wt% NaCl solution. The pH of the corrosive environment (3.5 wt% NaCl solution) was adjusted by 0.1M NaOH solution (for basic pH range) and 0.1M H₂SO₄ solution (for acidic pH range) at room temperature.

Before each electrochemical test, the specimens were kept at their open-circuit potentials (OCP) to establish the dynamic stabilization at the specimen/electrolyte interface. The impedance response were measured at the OCP potential with amplitude of 5 mV in a frequency range from 10 mHz to 10 kHz. The potentiodynamic polarization test were carried out from -300 to 300 mV with respect to OCP at scan rate of 1 mV/s. Salt spray tests were conducted based on ASTM-B117 standard for 50 hours using a WEISS TECHNIK device.

All the specimens were investigated firstly to assess their corroded surfaces (using a Leitz optical microscope and a Cambridge 260 scanning electron microscope) and mass loss measurements were also carried out after the salt spray tests. Before the mass loss measurements, the corroded samples were first rinsed well with distilled water and then acid pickled with a solution of 200g/L CrO₃ + 10 g/L AgNO₃ for one minute to remove all the corrosion products and residual salts from the surface [19]. The samples that were used for microstructural observations were first mechanically polished with abrasive papers up to 3000 grade and then chemically etched

in a solution containing 2.5ml acetic acid, 3g picric acid, 50ml ethanol and 5ml distilled water.

3. Results and Discussion

3.1. Effect of deformation technique on AZ91 magnesium alloy corrosion behavior

The microstructures of as-cast, extruded and SSEed specimens are shown in Fig. 1. As seen in Fig. 1a, the microstructure of as-cast samples consists of β (Mg₁₂Al₁₇) precipitations that are surrounded by eutectic (α + β) microconstituents distributed in the α -matrix. It has been reported that the formability of magnesium alloys is not much that they can exhibit high strain values which may be experienced by the material as a result of SSE process [20]. Thus, in order to enhance their formability, the as-cast specimens were first heat treated and then quenched in water at ambient temperature to eliminate β precipitates from the structure. The heat treated samples were then extruded at 415°C in order to achieve further improvement in the formability (before SSE process) as has been reported elsewhere [21]. The microstructure of extruded sample is

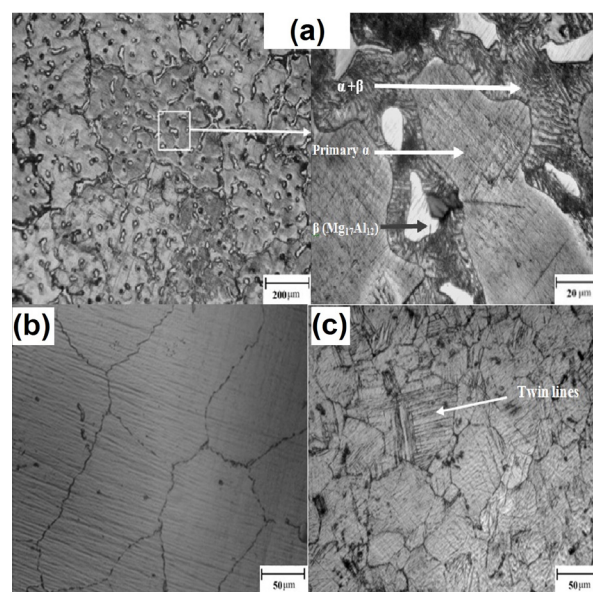


Fig. 1. OM micrographs from the surface of AZ91 Mg alloys: a) as-cast b) extruded c) SSEed.

illustrated in Fig. 1b indicating homogeneous α phase without any β precipitates that may have adverse effect on the alloy formability. As seen in Fig. 1c, SSE process led to decrease in the grain size and formation of twins in the microstructure of AZ91 magnesium alloy.

The AC responses (obtained in 3.5 wt% NaCl solution at room temperature) of AZ91 magnesium alloys that experienced different deformation processes are illustrated in Fig. 2. As seen, the AC responses of all the specimens include a capacitive loop at low frequency range followed by an inductive loop at high frequencies while their respective diameters varies for different samples. The diameter of the capacitive loop may be related to the charge transfer resistance (R_{ct}) at the electrode/solution interface. According to Fig. 2, the extruded sample has the highest value of R_{ct} (biggest capacitive loop diameter) which might be related to the elimination of β precipitates from the microstructure and remaining homogeneous α -phase (Fig. 1b) that exhibits better corrosion resistance. In addition, the R_{ct} -value of SSEed sample

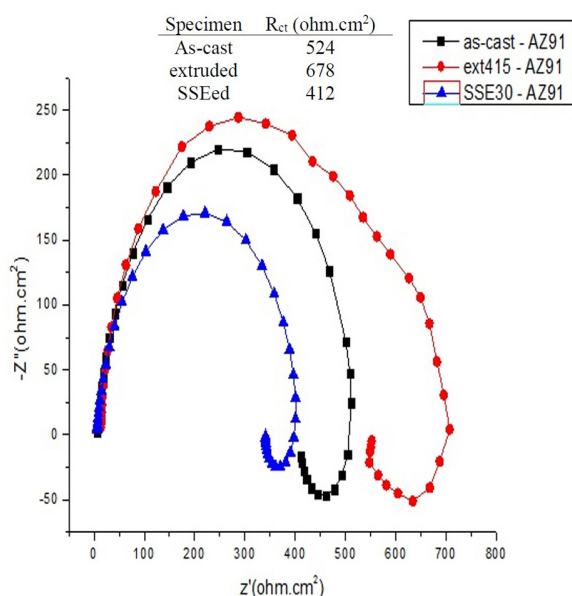


Fig. 2. AC responses of AZ91 Mg alloys in 3.5 wt% NaCl solution at room temperature: a) as-cast b) extruded c) SSEed.

is lower than that of as-cast one (compare their respective capacitive loop diameter) which indicates the adverse effect of the SSE technique on the corrosion behavior of AZ91 alloys. Such behavior would be related to the resulted fine grained active microstructure in the SSEed sample that also includes high energy areas, such as twins, as can be seen in Fig. 1c

The polarization curves related to differently prepared AZ91 magnesium alloys are presented in Fig. 3. As seen, the lowest and highest corrosion current densities (i_{corr}) are related to the extruded specimen and SSEed sample, respectively, which is in good accordance with the results obtained from EIS data. Such observations have been also reported for corrosion behavior of ECAPed (equal-channel angular pressed) AZ91D alloy in NaCl solution in which the enhanced corrosion has been related to the increase in the deformation induced crystalline defects that provides high energy areas suitable for promoted corrosion [15].

The surface morphologies of the as-cast,

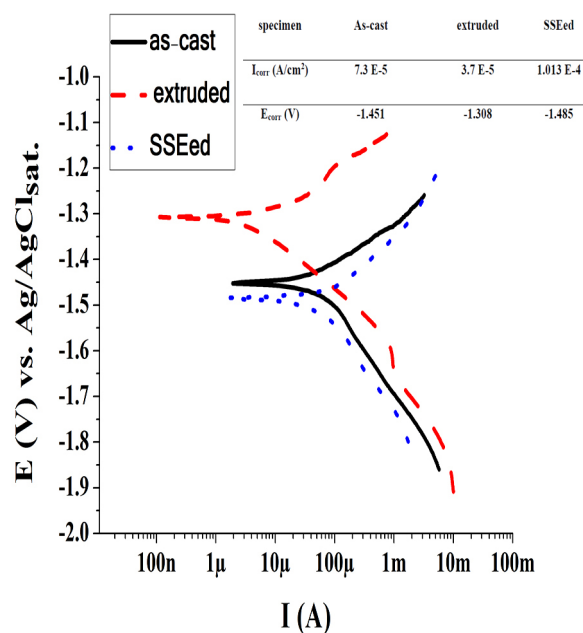


Fig. 3. Polarization curves of AZ91 alloys at room temperature: a) as-cast b) extruded c) SSEed.

extruded and SSEed samples, after the salt spray test, are presented in Fig. 4 a-c. As seen, more corrosion products are formed on the surface of SSEed samples, moreover, the surface of the extruded samples is covered with less corrosion products than the as-cast one. In addition, more compact corrosion products are formed on the surface of the samples that exhibits high corrosion resistance (Fig. 4 d-f). The obtained mass losses were used to estimate corrosion rate of the samples under the salt spray test condition based on equation (1).

$$\text{mpy}=534W/D.A.T \quad (1)$$

in which W is the mass loss (mg), D is the alloy density (g/cm^3), A is the surface area (in^2) and T is time in hours. The results of such calculations are presented in Table.2 which are in good accordance with the electrochemical test results, i.e. SSEed samples exhibit higher corrosion rates than the other ones.

3.2. Effect of temperature and pH on the corrosion behavior

The effect of solution temperature on the electrochemical impedance responses of

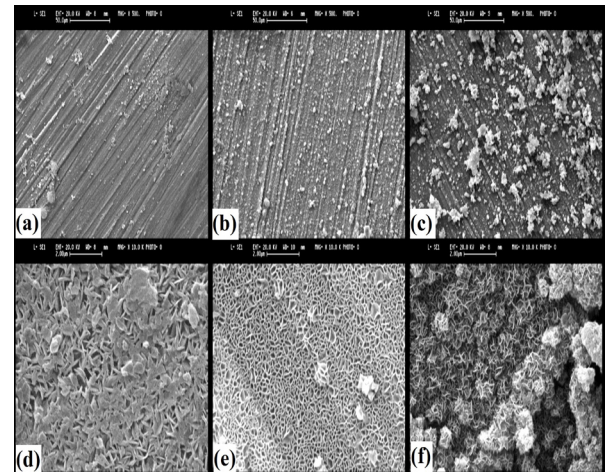


Fig. 4. SEM micrographs from the corroded surfaces of as- cast (a and d), extruded (b and e) and SSEed (c and f) samples after 50 h exposure in salt spray tests.

Table 2: Mass loss results after 50 h exposure in salt spray tests.

Sample	W1(g)	W2(g)	CR(mpy)
As-cast	1.3675	1.3598	63
Extruded	1.6255	1.6205	35
SSEed	1.1702	1.1627	82

SSEed magnesium AZ91 alloys are presented in Fig. 5. The equivalent circuit that was used to fit the experimental data is illustrated in Fig. 6 and the fitted results are presented

Fig. 5. AC responses of AZ91 Mg alloys in 3.5 wt% NaCl solution at various temperatures: a) as-cast and b) SSEed.

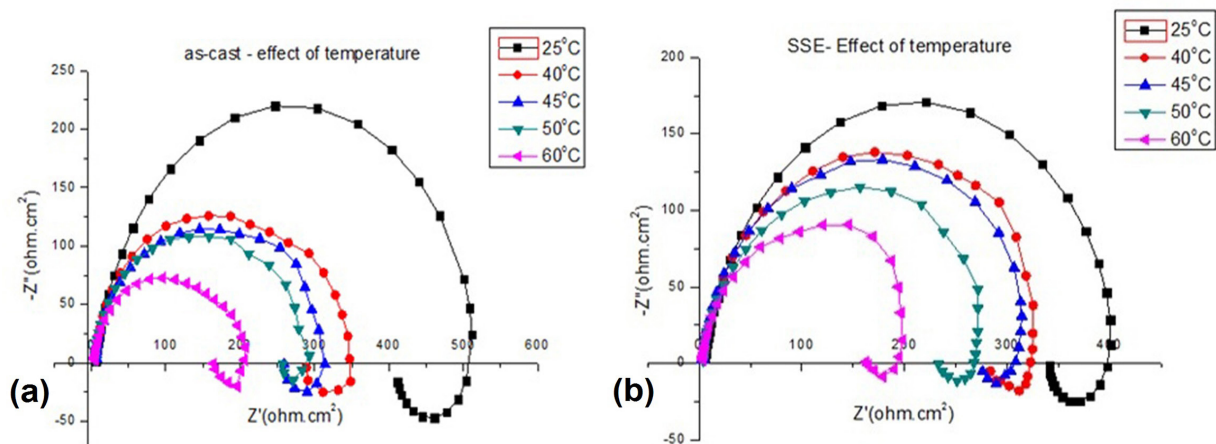
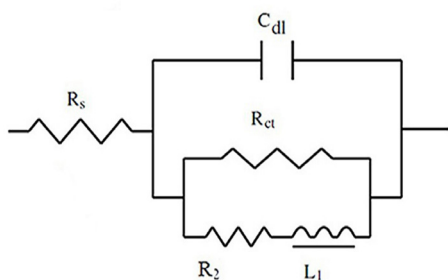
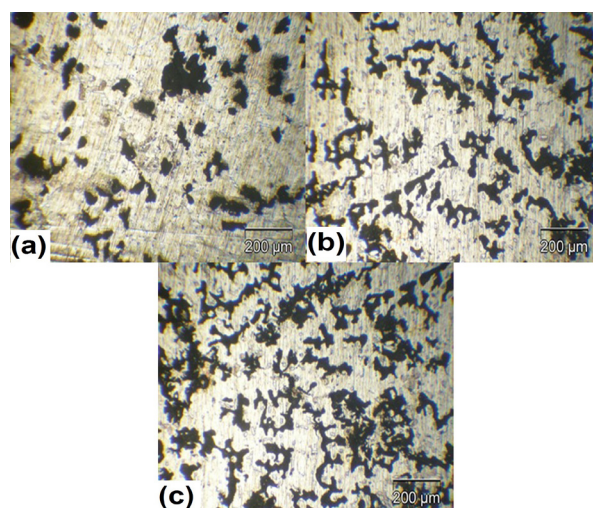
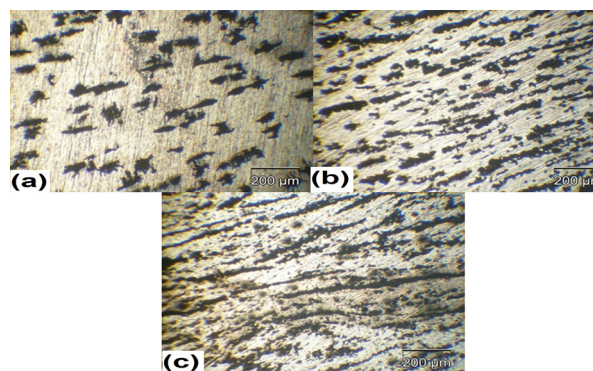


Table 3. The fitted results to the EIS data of as-cast and SSEed specimens in 3.5 wt% NaCl solutions at various temperatures.

	Temperature(°C)	R_s (ohm.cm ²)	$R_{p(ohm.cm^2)}$	$R_{ct(ohm.cm^2)}$	$L_{(H.cm^2)}$	Y_0	n	C(F)
As-cast	25	5.75	407	524	1675	$10^{-4} \times 0.284$	0.889	$10^{-5} \times 1.679$
	40	4.48	287	349	1405	$10^{-4} \times 0.212$	0.906	$10^{-5} \times 1.27$
	45	5.57	259	308	1064	$10^{-4} \times 0.214$	0.892	$10^{-5} \times 1.17$
	50	3.79	253	291	835	$10^{-4} \times 0.235$	0.897	$10^{-5} \times 1.32$
	60	3.598	156	187	637	$10^{-4} \times 0.162$	0.870	$10^{-5} \times 1.19$
SSEed	25	5.16	325	412	1525	$10^{-4} \times 0.151$	0.880	$10^{-6} \times 7.55$
	40	4.15	283	333	1538	$10^{-4} \times 0.144$	0.870	$10^{-6} \times 6.529$
	45	3.76	254	323	1420	$10^{-4} \times 0.147$	0.875	$10^{-6} \times 6.799$
	50	3.54	227	278	1192	$10^{-4} \times 0.193$	0.870	$10^{-6} \times 8.898$
	60	3.306	158	198	742	$10^{-4} \times 0.249$	0.875	$10^{-5} \times 1.156$

in Table. 3. In this circuit, R_s is the solution resistance, C_{dl} is the double-layer capacitance, R_{ct} is the charge-transfer resistance, R_2 is the polarization resistance and L_1 is an inductive element. The results show that increasing the solution temperature leads to decrease in the charge-transfer resistance (R_{ct}) of all the samples. The OM micrographs from the surface of the corroded specimens are shown in Fig. 7 and Fig. 8. As seen, the corroded areas (dark gray patches) are distributed more closely together as the solution temperature increases. In addition, the extrusion process caused corrosion to occur in a preferred direction parallel to the deformation axis that leads to have elongated pattern for corroded areas in the SSEed samples.

**Fig. 6.** The equivalent circuit used to fit the experimental EIS data.**Fig. 7.** OM micrographs from the corroded surface of as-cast AZ91 alloys at: a) 25°C °C, b) 40 °C °C and c) 60 °C °C.**Fig. 8.** OM micrographs from the corroded surface of SSEed AZ91 alloys at: a) 25 °C °C, b) 40 °C °C and c) 60 °C.

It has been reported that two chemical compounds, $Mg(OH)_2$ or mixed oxides of the Mg and Al, may be produced on the surface of such magnesium alloys depending on the pH value of the corrosive medium [22]. At acidic solutions, pH values around 2, β -phase plays an important role in the formation of the mixed oxides on the alloy surface while $Mg(OH)_2$ compound will precipitate on the alloy surface in alkaline solutions with pH values above 11 [23-25].

The effect of the solution pH on the impedance responses of SSEed magnesium

AZ91 alloys are presented in Fig. 9. As seen, impedance spectra are similar to those that were obtained at various temperatures including inductive and capacitive loops. The fitted results to the experimental data (Fig. 9) using equivalent circuit shown in Fig.6 are presented in Table 4. As seen, the R_{ct} -values increases as the pH level of the solution increases i.e. corrosion resistance of the samples are higher in alkaline media than in acidic ones. It may be related to the formation of an intact protective layer at high pH value [23]. The optical microscope micrographs from the corroded surfaces of as-cast and SSEed samples at

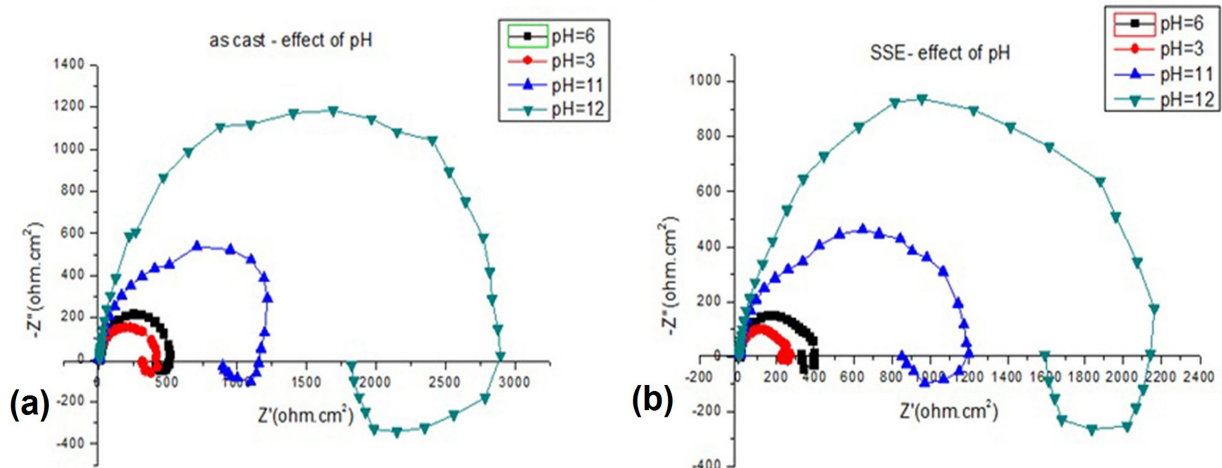


Fig. 9. AC responses of AZ91 Mg alloys in 3.5 wt% NaCl solution at different pH levels: a) as-cast and b) SSEed.

Table 4: The fitted results to the EIS data of as-cast and SSEed specimens in 3.5 wt% NaCl solutions at various pH levels at room temperature.

	pH	$R_s(\text{ohm.cm}^2)$	$R_p(\text{ohm.cm}^2)$	$R_{ct}(\text{ohm.cm}^2)$	$L_{(H.cm}^2)$	Y_0	n	C(F)
As-cast	3	3.65	312	427	1176	0.391×10^{-4}	0.876	2.19×10^{-5}
	6	5.75	407	524	1675	0.284×10^{-4}	0.889	1.679×10^{-5}
	11	5.1	896	1170	3850	0.232×10^{-4}	0.923	1.717×10^{-5}
	12	9.16	1878	2892	5600	0.708×10^{-5}	0.93	5.281×10^{-6}
SSEed	3	6.55	225	261	1028	0.156×10^{-4}	0.889	7.874×10^{-6}
	6	5.16	325	412	1525	0.151×10^{-4}	0.880	7.553×10^{-6}
	11	5.49	844	1195	3036	0.128×10^{-4}	0.89	7.635×10^{-6}
	12	6.14	1318	2197	3048	0.172×10^{-4}	0.93	1.345×10^{-5}

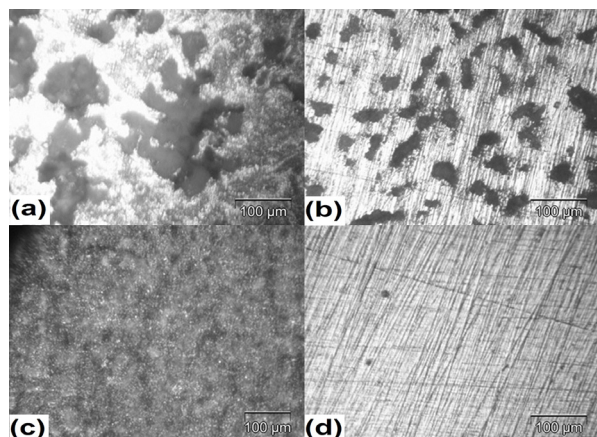


Fig. 10. Light microscope surface micrographs for AZ91 as-cast specimens showing effect of pH on corrosion morphology: a) pH=3, b) pH=6, c) pH=11 and d) pH=12.

various pH values are presented in Fig. 10 and Fig. 11, respectively. Again, more corrosion, in comparison to as-cast ones, occurred at preferential direction parallel to the extrusion axis in the SSEed samples; in addition, more

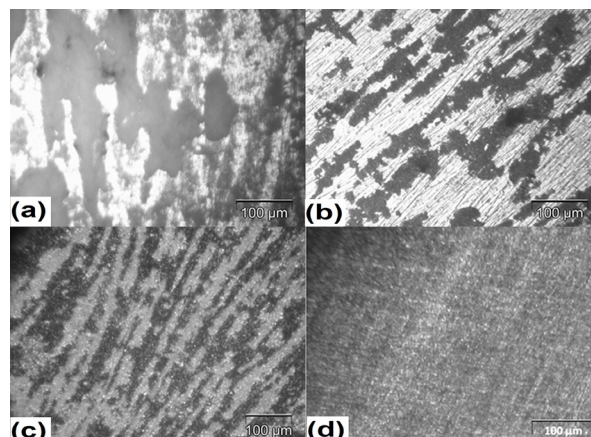


Fig. 11. Light microscope surface micrographs for AZ91 SSEed specimens showing effect of pH on corrosion morphology: a) pH=3, b) pH=6, c) pH=11 and d) pH=12.

corroded areas (dark patches) are created at low pH (acidic) solutions in both as-cast and extruded samples.

Potentiodynamic polarization responses of the samples, prepared at various experimental

Table 5: Electrochemical parameters obtained by potentiodynamic technique for as-cast and SSEed AZ91 in 3.5 wt% NaCl at various temperatures.

	Temperature (°C)	E_{corr} (V) vs. Ag/AgCl _{sat}	i_{corr} (A/cm ²)	CR (mm/y)
As-cast	25	-1.343	6.27×10^{-6}	0.145
	40	-1.455	8.107×10^{-5}	1.875
	60	-1.527	1.419×10^{-4}	3.26
SSEed	25	-1.409	1.76×10^{-5}	0.407
	40	-1.486	$10^{-5} \times 3.58$	0.828
	60	-1.532	$10^{-5} \times 6.389$	1.478

Table 6: Electrochemical parameters obtained by potentiodynamic technique for as-cast and SSEed AZ91 in 3.5 wt% NaCl at different pH levels.

	pH	E_{corr} (V) vs. Ag/AgCl _{sat}	i_{corr} (A/cm ²)	CR (mm/y)
As-cast	3	-1.493	1.88×10^{-4}	4.26
	6	-1.451	6.47×10^{-5}	1.463
	11	-1.433	4.75×10^{-5}	1.074
	12	-1.363	2.611×10^{-5}	0.588
SSEed	3	-1.522	2.037×10^{-4}	4.43
	6	-1.485	7.013×10^{-5}	1.605
	11	-1.452	4.66×10^{-5}	1.05
	12	-1.403	2.064×10^{-5}	0.466

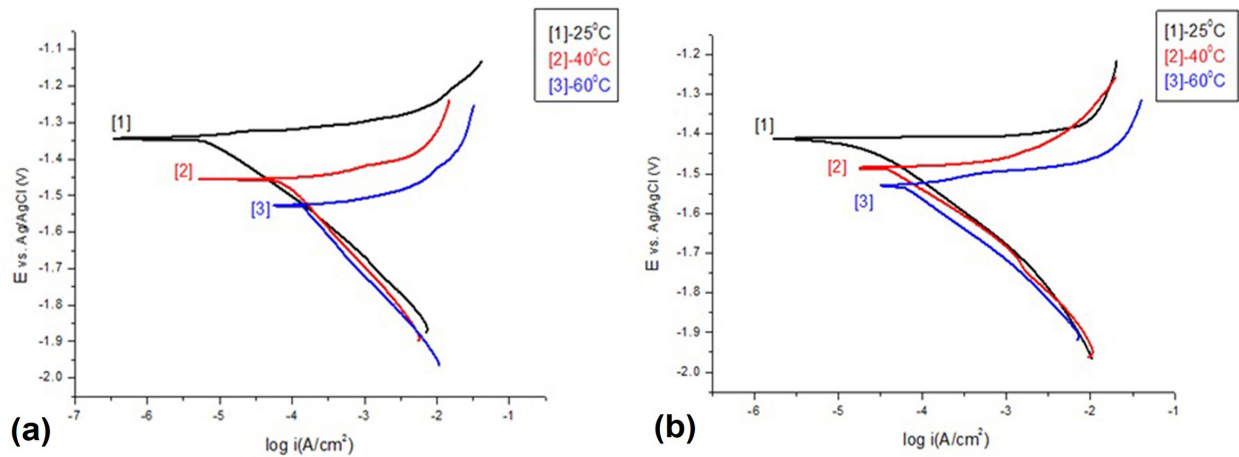


Fig. 12. Polarization curves of a) as-cast and b) SSEed AZ91 alloys in 3.5wt% NaCl solution at various temperatures.

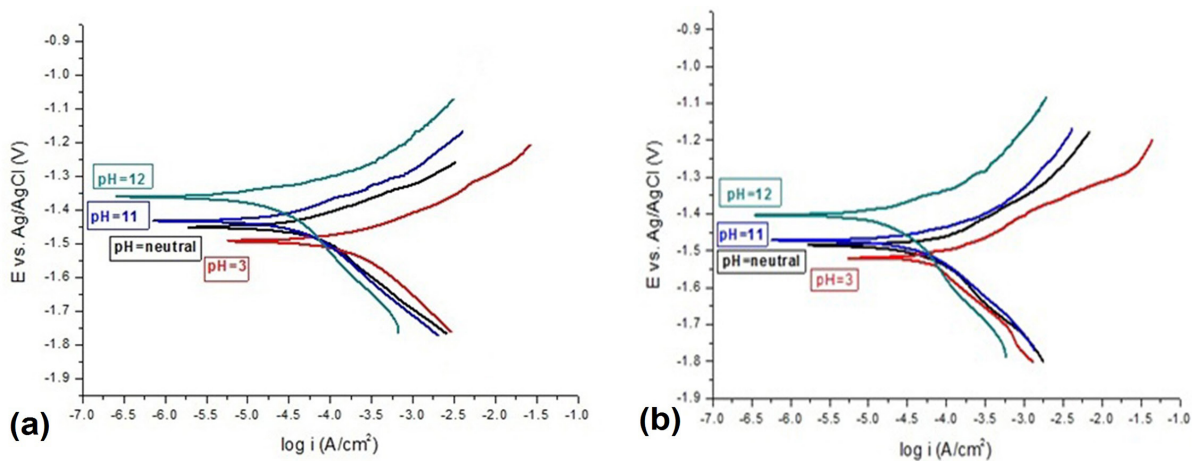


Fig. 13. Polarization curves of a) as-cast and b) SSEed AZ91 alloys in 3.5wt% NaCl solution at various pH levels.

conditions, are shown in Fig. 12 and Fig. 13 and the related data are presented in Table.5 and Table.6, respectively. The corresponding corrosion rates (in mm/year) were calculated using equation (2) in which i_{corr} is corrosion current density ($\mu\text{A}/\text{cm}^2$), M is molecular weight (g/mol), n is the number of electrons and D is the density ($\text{g}\cdot\text{cm}^{-3}$).

$$\text{CR} = (3.28 \times 10^{-3}) i_{\text{corr}} (M/nD) \quad (2)$$

As seen, the corrosion potential becomes more negative and corrosion current increases by increasing the temperature and decreasing the pH of the solution in both as-cast and SSEed samples. This type of behavior is in good accordance with the EIS test results

that showed a decrease in the charge transfer resistance as the environmental factors (solution pH and temperature) altered in the same way.

4. Conclusion

Simple shear extrusion has adverse effect on the corrosion behavior on as-cast AZ91 magnesium alloys. The corrosion performance of the SSEed samples got worsens as a result of increasing the temperature and degree of solution acidity. In addition, the corrosion occurred in preferred direction parallel to the deformation axis leading to have elongated areas that were corroded at the surface of SSEed specimens.

Reference

- [1]H. A. beni, M. Alizadeh, M. Ghaffari and R. Amini, *Composites Part B: Engineering*. 58 (2014) 438–442.
- [2]Y. Miyahara, K. Matsubara, Z. Horita and T. G. Langdon, *Metallurgical and Materials Transaction A*. 36A (2005) 1705-1711.
- [3]R. J. Hellmig, M. Janecek, B. Hadzima, O. V. Gendelman, M. Shapiro, X. Molodova, A. Springer and Y. Estrin, *Materials Transactions*. 49 (2008) 31-37.
- [4]R. Jahadi, M. Sedighi and H. Jahed, *Materials Science and Engineering: A*. 593 (2014) 178–184.
- [5]K. Edalati, M. Ashidab, Z. Horita, T. Matsui and H. Kato, *Wear*. 310 (2014) 83–89.
- [6]L. Ghalandari, M. M. Mahdavian and M. Reihanian, *Materials Science and Engineering: A*. 593 (2014) 145–152.
- [7]N. Pardis and R. Ebrahimi, *Materials Science and Engineering A*. 527 (2009) 355-360.
- [8]S. Mathieu, C. Rapin, J. Steinmetz and P. Steinmetz, *Corrosion Science*. 45 (2003) 2741-2755.
- [9]J. Chen, J. Wang, E. Han, J. Dong and W. Ke, *Electrochimica Acta*. 52 (2007) 3299–3309.
- [10]L. Wang, B. P. Zhang and T. Shinohara, *Materials and Design*. 31 (2010) 857–863.
- [11]S. Gollapudi, *Corros. Sci.* 62 (2012) 90–94.
- [12]Z. Pu, G. L. Song, S. Yang, J. C. Outeiro, O. W. D. Jr., D. A. Puleo and I. S. Jawahir, *Corros. Sci.* 57 (2012) 192–201.
- [13]N. N. Aung and W. Zhou, *Corrosion Science*. 52 (2010) 589–594.
- [14]K. D. Ralston, N. Birbilis, M. K. Cavanaugh, M. Weyland, B. C. Muddle and R. K. W. Marceau, *Electrochim. Acta*. 55 (2010) 7834–7842.
- [15]D. Song, A. B. Ma, J. H. Jiang, P. H. Lin, D. H. Yang and J. F. Fan, *Corrosion Science*. 53 (2011) 362-373.
- [16]Y. Song, E.-H. Han, K. Dong, D. Shan, C. D. Yim and B. S. You, *Corrosion Science*. 88 (2014) 215–225.
- [17]N. D. Nam, M. Mathesh, T. V. Le and H. T. Nguyen, *Journal of Alloys and Compounds*. 616 (2014) 662–668.
- [18]L. Xiaoyan, L. Mingzhao, F. Liuqun, W. Haiyan, F. Chong and M. Hua, *Rare Metal Materials and Engineering*. 43 (2014) 278-282.
- [19]Y. Tian, L. Yang, Y. Li, Y. Wei, L. Hou and R. Murakami, *Trans Nonferrous Met Soc China*. 21 (2011) 912-920.
- [20]N. B. Tork, N. Pardis and R. Ebrahimi, *Materials Science and Engineering: A*. 560 (2013) 34–39.
- [21]M. Avedesian and H. Baker, *ASM specialty Handbook, Magnesium and Magnesium alloy*, ASM international, 1999.
- [22]C. Brun, J. Pagetti and J. Talbot, *Mem. Sci. Rev. Metall.* 73 (1976) 659-668.
- [23]R. Ambat, N. N. Aung and W. Zhou, *Journal of Applied Electrochemistry*. 30 (2000) 865-874.
- [24]S. Alsagabi, J. Ninlachart, K. S. Raja and I. Charit, *Journal of Materials Engineering and Performance*. 25 (2016) 2364-2374.
- [25]N. Dinodi and A. N. Shetty, *Surface Engineering and Applied Electrochemistry*. 50 (2014) 149-156.